

# The metabolic balance at two contrasting sites in the Southern Ocean: The iron-fertilized Kerguelen area and HNLC waters

Dominique Lefèvre<sup>a,\*</sup>, Catherine Guigue<sup>a</sup>, Ingrid Obernosterer<sup>b,c</sup>

<sup>a</sup>Aix-Marseille Université, CNRS, LMGEM-UMR 6117, Laboratoire de Microbiologie, Géochimie et Ecologie Marines, Campus de Luminy—Case 901, 13288 Marseille cedex 9, France

<sup>b</sup>Université Pierre et Marie Curie—Paris6, Laboratoire ARAGO, Avenue Fontaulé, BP44, F66650 Banyuls-sur-Mer, France

<sup>c</sup>CNRS, UMR7621, Laboratoire d'Océanographie Biologique de Banyuls, Avenue Fontaulé, BP44, F-66650 Banyuls-sur-Mer, France

Accepted 11 December 2007

Available online 14 March 2008

## Abstract

We investigated the balance between autotrophic and heterotrophic processes during the third month of an intense phytoplankton bloom induced by natural iron enrichment above the Kerguelen plateau (Southern Ocean). Gross (GCP)- and net community production (NCP) and dark community respiration (DCR) were determined using concurrent measurements of dissolved oxygen ( $O_2$ ) and total carbon dioxide ( $TCO_2$ ) evolution in light- and dark-bottle incubations. Experiments were carried out during four visits to one station located in the core of the phytoplankton bloom and at a high-nutrient low-chlorophyll (HNLC) site. Within the bloom, euphotic zone (around 45 m) integrated fluxes of NCP were high during the first three visits, varying between 64 and 92  $mmol O_2 m^{-2} d^{-1}$  and between  $-43$  and  $-105 mmol TCO_2 m^{-2} d^{-1}$ . On the last visit, however, fluxes of NCP indicated a shift from autotrophic to heterotrophic plankton metabolism, with a net consumption of  $O_2$  ( $-72 mmol O_2 m^{-2} d^{-1}$ ) and a net production of  $TCO_2$  ( $64 mmol TCO_2 m^{-2} d^{-1}$ ). This shift was accompanied by a 5-fold increase in DCR, while integrated fluxes of GCP remained similar throughout the sampling period ( $110 \pm 21 mmol O_2 m^{-2} d^{-1}$  and  $-100 \pm 27 mmol TCO_2 m^{-2} d^{-1}$ ). Fluxes of NCP integrated to the euphotic zone (around 100 m) were low at a typical HNLC site, ranging from 0 to 5  $mmol O_2 m^{-2} d^{-1}$  during three visits. These data suggest that above the Kerguelen plateau organic matter production largely exceeded its immediate respiration, while at the HNLC site autotrophic and heterotrophic processes are close to balance. During the spring phytoplankton bloom above the Kerguelen plateau, a substantial part of primary production is therefore potentially available for mesozooplankton grazing and export, or respiration at a different time period.

© 2008 Elsevier Ltd. All rights reserved.

**Keywords:** NCP; HNLC; Kerguelen plateau

## 1. Introduction

The Southern Ocean is continuously supplied with high concentrations of major inorganic nutrients, thus holding a large potential for primary production and atmospheric carbon dioxide uptake. Phytoplankton biomass, however, is low across large parts of the Southern Ocean, an observation that can be explained by the growth-limiting concentrations of dissolved iron (DFe) (Boyd et al., 2000; Gervais et al., 2002; Coale et al., 2004). Exceptions to this overall low primary production are the annually occurring

phytoplankton blooms found in distinct areas (Sullivan et al., 1993). These phytoplankton blooms are predominantly regulated by iron from shelf sediments or sea-ice melt, or mixing with iron-rich upper circumpolar deep water (Hiscock, 2004). The build-up of phytoplankton biomass in the surface waters of the Southern Ocean has been followed primarily using satellite observations, which leave important questions regarding the uptake and sequestration of atmospheric carbon dioxide unresolved.

Several recent experiments performed in the Atlantic (EisenEx, Gervais et al., 2002; SOFeX, Coale et al., 2004) and Pacific (SOIREE, Gall et al., 2001; SEEDS, Kudo et al., 2005) sectors of the open Southern Ocean have studied the impact of iron fertilization on phytoplankton

\*Corresponding author.

E-mail address: [dominique.lefevre@univmed.fr](mailto:dominique.lefevre@univmed.fr) (D. Lefèvre).

productivity and carbon sequestration *in situ*. In all these experiments, intense phytoplankton blooms evolved upon mesoscale iron addition to surface waters; however, carbon export was only slightly higher (SOFeX, Buesseler et al., 2004) or similar (SOIREE, Boyd et al., 2000) to that in waters surrounding the iron-fertilized patch. This was attributed to the dilution of the iron-fertilized patch with surrounding waters and to the short time period (weeks) over which carbon export was followed. Another process that determines the amount of carbon export is the biological mineralization of photosynthetically fixed carbon within the upper water column.

Net community production (NCP), the balance between gross community production (GCP) and respiration, sets an upper limit to the export of phytoplankton production. NCP, defined as the rate of the net storage of organic matter, is often linked to the structure of the planktonic food web. Planktonic systems dominated by the microbial food web are generally characterized by the rapid mineralization of carbon and nutrients, and hence low NCP. Classical food webs, by contrast, appear to dominate in systems where phytoplankton biomass build-up and carbon export are relatively high. Phytoplankton blooms in the Southern Ocean have been taken as examples for the latter case (Karl, 1993; Pomeroy and Deibel, 1986) indicating their potential importance for carbon sequestration.

The Kerguelen plateau is located in the Indian Sector of the Southern Ocean, between the Polar Front to the north (Park and Gambéroni, 1997; Park et al., 1998) and the Fawn Trough Current to the south (McCartney and

Donohue, 2007; Roquet et al., 2008), and it constitutes a major barrier to the eastward flowing Antarctic Circumpolar Current (ACC) (Park et al., 1991, 1993). Massive phytoplankton blooms occur annually above the Kerguelen plateau. Natural fertilization of surface waters by iron and major nutrients from below was suggested to initiate these blooms at the onset of spring (Blain et al., 2001), a hypothesis that was tested during the *KErguelen Ocean and Plateau compared Study* (KEOPS) cruise in January–February 2005. Our objective within the KEOPS-project, was to study the NCP that is potentially important for the net absorption of atmospheric carbon dioxide as well as the export of organic carbon into the interior of the ocean.

## 2. Methods

### 2.1. Study sites

The study was performed in the phytoplankton bloom above the Kerguelen plateau and in the surrounding high-nutrient low-chlorophyll (HNLC) waters (Fig. 1) (Blain et al., 2007). Composite MODIS and MERIS satellite images indicated the onset of the Kerguelen bloom roughly 2 months prior to the start of the KEOPS-cruise (January 19–February 13, 2005) and its collapse at the end of February. The two stations considered herein were located above the Kerguelen plateau in the core of the phytoplankton bloom (station A3, 527 m) and off the plateau in HNLC waters (station C11, 2500 m). Station A3 was visited five times during the cruise, following the bloom from its peak to its

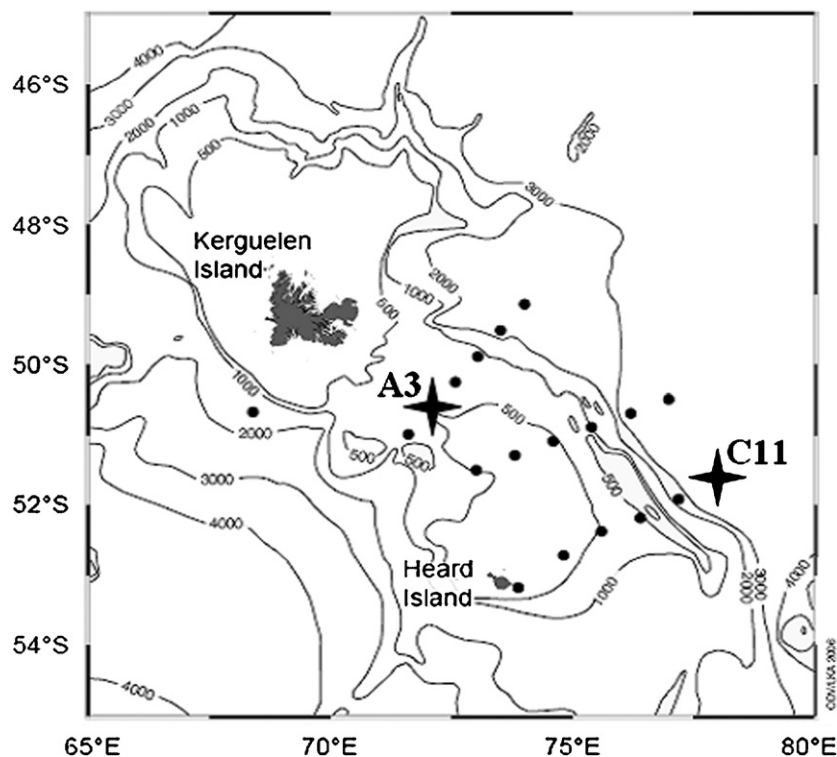


Fig. 1. Study area above the Kerguelen plateau, with stations A3 and C11 indicated on transects (⊕).

Table 1  
Brief description of the hydrological context of the study sites

Station	Date	Zm (m)	Ze (m)	Temperature Zm (°C)	NO <sub>3</sub> <sup>-</sup> + NO <sub>2</sub> <sup>-</sup> (μM)	NH <sub>4</sub> <sup>+</sup> (μM) <sup>a</sup>	PO <sub>4</sub> <sup>3-</sup> (μM) <sup>a</sup>	Si(OH) <sub>4</sub> (μM) <sup>a</sup>	DFe (nM) <sup>b</sup>	Chlorophyll <i>a</i> (μg dm <sup>-3</sup> ) <sup>c</sup>
A3-1	January 19	52 ± 12	42	3.5	22.7 ± 0.4	0.25 ± 0.03	1.45 ± 0.11	1.96 ± 0.23	0.13	1.6 ± 0.5
A3-3	January 24	51 ± 14	40	3.7	24.9 ± 0.3	0.32 ± 0.10	1.54 ± 0.04	1.55 ± 0.12	0.07	1.4 ± 0.6
A3-4	February 3	79 ± 20	46	3.6	23.2 ± 0.0	0.75 ± 0.02	1.77 ± 0.28	1.82 ± 0.23	0.11	1.5 ± 0.1
A3-5	February 12	84 ± 19	44	3.9	22.1 ± 0.4	0.71 ± 0.03	1.78 ± 0.11	1.20 ± 0.15	0.13	1.0 ± 0.1
C11-1	January 26	73 ± 13	98	1.8	30.7 ± 0.2	0.62 ± 0.17	2.09 ± 0.04	24.83 ± 0.33	0.095	0.2 ± 0.1
C11-2	January 28	73 ± 13	98	1.8	27.8 ± 0.4	0.43 ± 0.05	2.23 ± 0.11	25.40 ± 0.20	n.d.	0.2 ± 0.1
C11-3	February 05	56 ± 1	123	1.9	29.0 ± 0.3	0.35 ± 0.01	2.10 ± 0.00	25.23 ± 0.58	n.d.	0.2 ± 0.03

The mixed layers are the mean ± SD of all CTD casts performed during the occupation of the stations.

Zm—mixed layer depth, Ze—euphotic zone, NO<sub>3</sub><sup>-</sup> + NO<sub>2</sub><sup>-</sup>.

n.d.—not determined.

<sup>a</sup>Mean values ± SD for the mixed layer depth. Mosseri et al. (2008).

<sup>b</sup>Mean values for the mixed layer depth. Blain et al. (2008).

<sup>c</sup>Mean values ± SD for the upper 100 m. Uitz et al. (2008).

decline. The parameters presented herein were determined during the first (A3-1), third (A3-3), fourth (A3-4), and fifth (A3-5) visit (Table 1). Station C11 was visited three times (C11-1, C11-2, C11-3).

Collection of seawater for dark community respiration (DCR) and NCP was achieved using General Oceanics 12 dm<sup>3</sup> Niskin bottles mounted on a rosette equipped with a SeaBird SBE19+ CTD, a Chelsea fluorometer, a Wetlab transmissiometer and a Biosperical PAR sensor. Inorganic nutrients were measured aboard the R.V. *Marion Dufresne* using methods adapted from Tréguer and LeCorre (1975).

## 2.2. GCP, DCR, and NCP

Rates of GCP, DCR, and NCP were estimated from changes in the dissolved oxygen (O<sub>2</sub>) and total carbon dioxide (TCO<sub>2</sub>) concentration over 24-h incubations carried out *in vitro* in on-deck incubations. Rates were measured at 1%, 4%, 8%, 25%, 50%, and 100% of surface photosynthetically active radiation (PAR) levels, using optical density filters (Nickel). Water samples were collected at the depths corresponding to the respective *in situ* PAR intensities. Therefore, a PAR-depth profile was performed at solar noon the day prior to the incubation experiments. Incubations were performed at sea-surface temperature that corresponded to the temperature in the euphotic zone, except for station C11 where the euphotic zone exceeded the mixed layer depth (MLD) (Table 1). Three sets of four replicates were collected in 125-cm<sup>3</sup> borosilicate glass bottles. One set of samples was fixed immediately to measure the O<sub>2</sub> and TCO<sub>2</sub> concentrations at time 0; the second set was incubated for 24 h in the dark and the remaining set was incubated at a set percentage of incident light. Dissolved O<sub>2</sub> concentration was measured using an automated high-precision Winkler titration system linked to a photometric end-point detector (Williams and Jenkinson, 1982). The TCO<sub>2</sub> concentration was measured using a home-built extraction unit, based on the single-operator multi-parameter metabolic analyzer (SOMMA)

coupled to a CO<sub>2</sub> coulometer (model 5011; UIC<sup>®</sup> Coulometrics) and a personal computer (Johnson et al., 1993). The TCO<sub>2</sub> system was calibrated as described in DOE (1994), and drift was checked using certified reference material (provided by A.G. Dickson, Scripps Institution of Oceanography). Pooled standard deviations for the O<sub>2</sub> titrations were 0.24, 0.32, and 0.36 μmol O<sub>2</sub> dm<sup>-3</sup> for time zero, 24-h dark and 24-h light incubations, respectively. Pooled standard deviations of TCO<sub>2</sub> titrations were 1.5, 1.2, and 1.3 μmol TCO<sub>2</sub> dm<sup>-3</sup> for time zero, 24-h dark and 24-h light incubations, respectively. These pooled standard deviations are in the range of those previously reported (Robinson and Williams, 1999). The overall coefficient of variation for O<sub>2</sub> and TCO<sub>2</sub> titrations was 0.06%.

NCP was calculated as the difference in the O<sub>2</sub> or TCO<sub>2</sub> concentration between “light” incubated samples and “time 0” samples. DCR was calculated as the difference between “dark” incubated samples and “time 0” samples. DCR rates are expressed as a negative O<sub>2</sub> rate and a positive TCO<sub>2</sub> rate. GCP is the difference between NCP and DCR, GCP rates are expressed as a negative TCO<sub>2</sub> rate and a positive O<sub>2</sub> rate (Gaarder and Gran, 1927). The precision of the mean O<sub>2</sub> rate was ± 0.2 μmol O<sub>2</sub> dm<sup>-3</sup> d<sup>-1</sup>, and the precision of the mean TCO<sub>2</sub> rate was ± 0.9 μmol TCO<sub>2</sub> dm<sup>-3</sup> d<sup>-1</sup> estimated using the standard error from the analysis of quadruple samples sets.

Photosynthetic (PQ) and respiratory quotients (RQ) were calculated as GCP[O<sub>2</sub>]/GCP[TCO<sub>2</sub>] and DCR[TCO<sub>2</sub>]/DCR[O<sub>2</sub>], respectively, and the standard error of the quotients was determined from: SE of X/Y = 1/Y<sup>2</sup>(Y<sup>2</sup>x<sup>2</sup> + X<sup>2</sup>y<sup>2</sup>)<sup>0.5</sup> where X and Y are means, x is the standard error of X and y is the standard error of Y. PQ and RQ were calculated for the six depths sampled. A mean PQ and RQ was subsequently calculated for each visit to station A3. PQ and RQ were not calculated at station C11 because TCO<sub>2</sub> rates were below the detection limit (data not shown). Therefore, we applied an RQ of 1 (mean of observed values at station A3) and a PQ of 1.2 at station C11 (Williams and Robertson, 1991).

### 3. Results

#### 3.1. Hydrography and chlorophyll

Above the Kerguelen plateau, at station A3 the MLD was highly variable over time due to internal wave activity (Park et al., 2008). During the four visits to station A3, the mean MLD ranged from 51 to 84 m (Table 1 and Fig. 2). At station C11, the mean MLD varied between 56 and 73 m. Measurements of *in situ* irradiance indicated that the attenuation of solar radiation remained relatively constant during the four occupations of station A3 with euphotic zone depths varying between 40 and 46 m (Table 1). The temperature in the MLD varied between 3.5 and 3.9 °C at station A3 and was 1.8 °C in the MLD of station C11 (Table 1).

Chlorophyll *a* concentrations, averaged over the upper 100 m of the water column, ranged between 1 and 1.6  $\mu\text{g dm}^{-3}$  at station A3, while phytoplankton biomass was considerably lower at the HNLC site C11 (0.2  $\mu\text{g dm}^{-3}$ ; Table 1) (Mosseri et al., 2008). Concentrations of nitrate +

nitrite were  $23.2 \pm 0.6$  and  $29.2 \pm 0.5 \mu\text{M}$  in the mixed layer at stations A3 and C11, respectively. Similar concentrations of  $\text{PO}_4^{3-}$  (1.8–2.1  $\mu\text{M}$ ) were detectable above and off the plateau (Mosseri et al., 2008). In surface waters, DFe concentrations were in the low nanomolar range ( $\approx 0.1 \text{ nM}$ ) at all stations, but DFe increased rapidly with depth above the Kerguelen plateau (Blain et al., 2008).

#### 3.2. GCP, DCR, and NCP

Above the Kerguelen plateau at station A3, GCP varied between 0.2 and 7.3  $\mu\text{mol O}_2 \text{ dm}^{-3} \text{ d}^{-1}$  and between  $-0.4$  and  $-10 \mu\text{mol TCO}_2 \text{ dm}^{-3} \text{ d}^{-1}$  during the four visits (Fig. 3) and GCP was substantially lower at the HNLC site C11 (0.1–0.8  $\mu\text{mol O}_2 \text{ dm}^{-3} \text{ d}^{-1}$ ) (Fig. 4). DCR was relatively constant throughout the euphotic zone and revealed minor differences among the first three visits to station A3 (mean  $\pm$  SD  $-1.0 \pm 0.4 \mu\text{mol O}_2 \text{ dm}^{-3} \text{ d}^{-1}$  and  $0.8 \pm 0.6 \mu\text{mol TCO}_2 \text{ dm}^{-3} \text{ d}^{-1}$ ,  $n = 18$ ) (Fig. 3). During the fifth visit, however, DCR increased substantially, yielding a mean euphotic zone respiration rate of

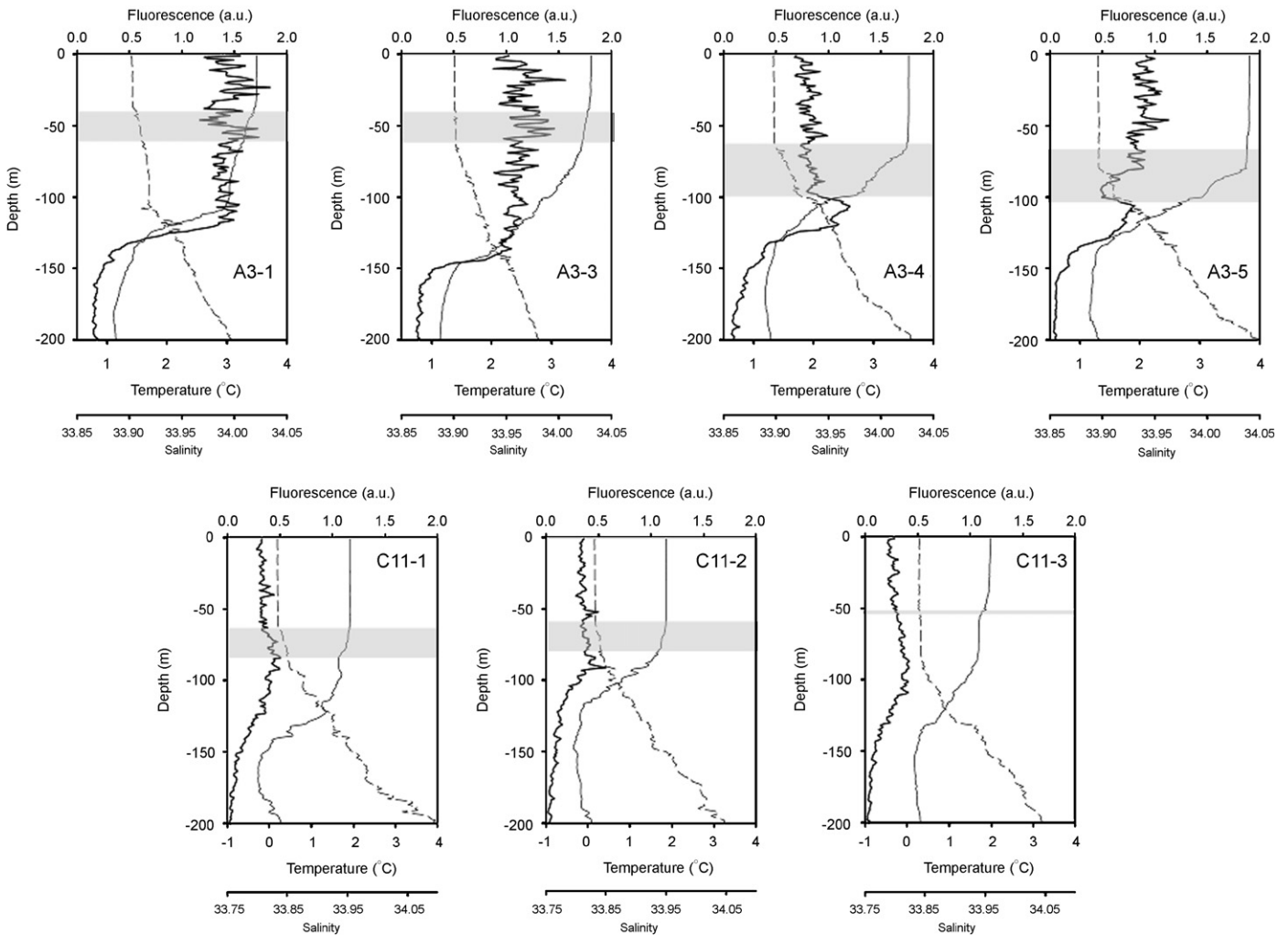


Fig. 2. Depth profiles of temperature (°C, —), salinity (---) and fluorescence (a.u., —) during four visits at station A3 and three visits at station C11. The range of the mixed-layer depth (mean  $\pm$  SD) is indicated for each visit as the shadowed area (■).

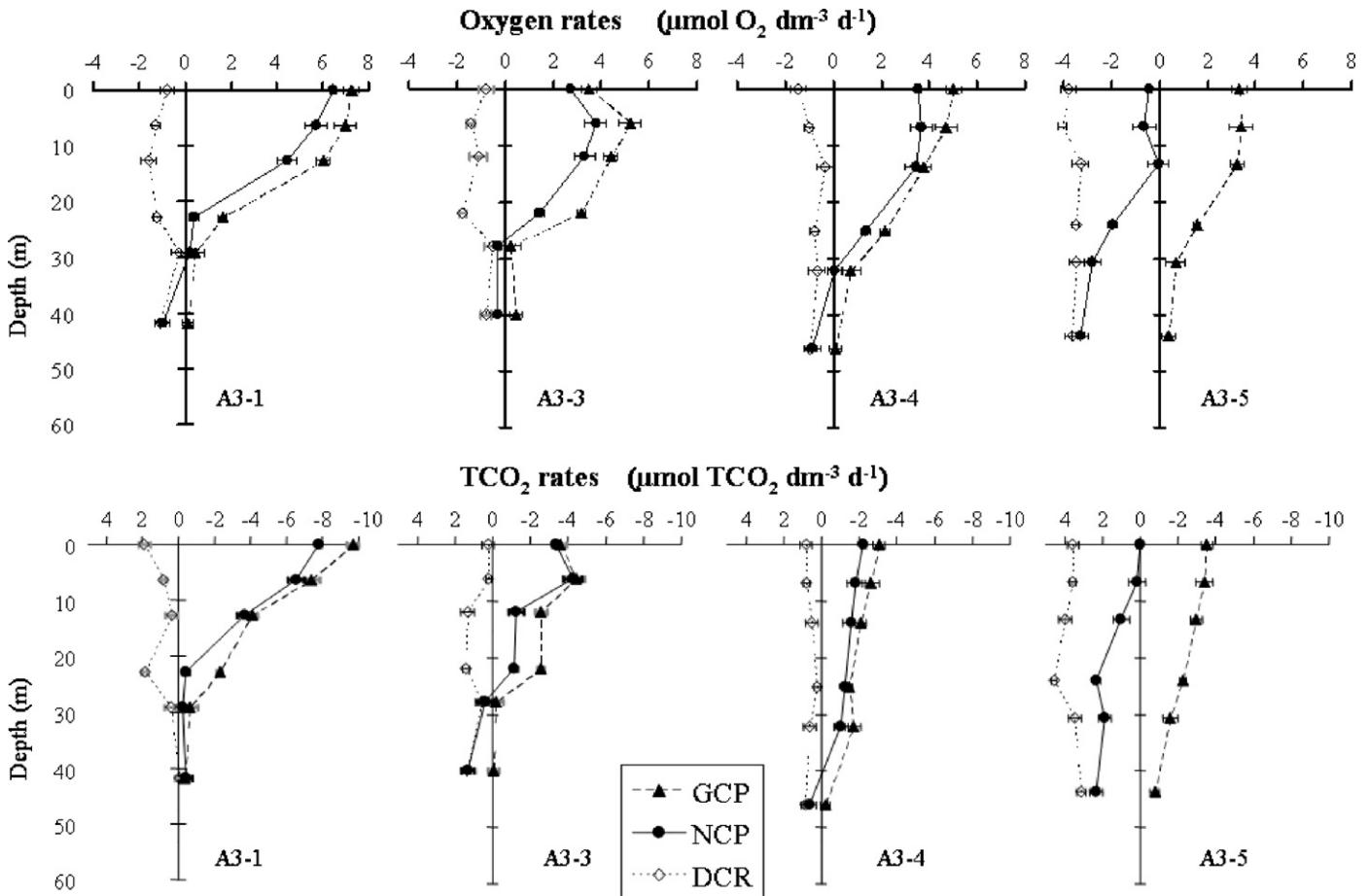


Fig. 3. Depth profiles of gross community production (GCP,  $\blacktriangle$ ), dark community respiration (DCR,  $\cdots\diamond$ ) and net community production (NCP,  $\bullet$ ) as determined from *in vitro* changes of  $O_2$  (upper panels) and  $TCO_2$  concentrations (bottom panels, note that  $TCO_2$  rates scale are in reverse order) during four visits at station A3. Mean values  $\pm$  SE are given.

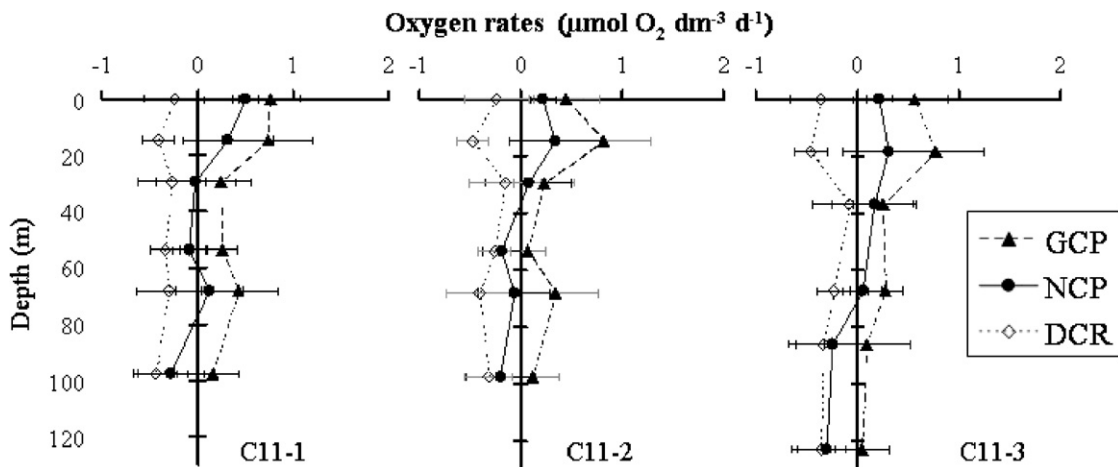


Fig. 4. Depth profiles of gross community production (GCP,  $\blacktriangle$ ), dark community respiration (DCR,  $\cdots\diamond$ ) and net community production (NCP,  $\bullet$ ) as determined from *in vitro* changes of  $O_2$  during three visits at station C11. Mean values  $\pm$  SE are given.

$-3.6 \pm 0.3 \mu\text{mol } O_2 \text{ dm}^{-3} \text{ d}^{-1}$  and  $3.7 \pm 0.5 \mu\text{mol } TCO_2 \text{ dm}^{-3} \text{ d}^{-1}$  ( $n = 6$ ). At the HLNC site C11, DCR revealed small variability within depths and among visits (mean  $\pm$  SD  $-0.3 \pm 0.1 \mu\text{mol } O_2 \text{ dm}^{-3} \text{ d}^{-1}$ ,  $n = 18$ ) (Fig 4). NCP was highest during the first visit to station A3 with maximum

values close to the sea surface of  $6.5 \mu\text{mol } O_2 \text{ dm}^{-3} \text{ d}^{-1}$  and  $-7.8 \mu\text{mol } TCO_2 \text{ dm}^{-3} \text{ d}^{-1}$ . NCP decreased during the third and fourth visits to subsurface values of  $3.8 \mu\text{mol } O_2 \text{ dm}^{-3} \text{ d}^{-1}$  and  $-4.2 \mu\text{mol } TCO_2 \text{ dm}^{-3} \text{ d}^{-1}$  (Fig. 3). During the fifth visit to station A3 a drastic shift

in NCP was detectable, with mean ( $\pm$ SD) values for the euphotic zone of  $-1.5 \pm 1.3 \mu\text{mol O}_2 \text{ dm}^{-3} \text{ d}^{-1}$  and  $1.3 \pm 1.0 \mu\text{mol TCO}_2 \text{ dm}^{-3} \text{ d}^{-1}$  ( $n = 6$ ) (Fig. 3). At the HNLC site C11, NCP varied between  $-0.30$  and  $0.50 \mu\text{mol O}_2 \text{ dm}^{-3} \text{ d}^{-1}$  (Fig. 4).

GCP integrated to the euphotic zone amounted to  $135 \pm 14 \text{ mmol O}_2 \text{ m}^{-2} \text{ d}^{-1}$  and  $-138 \pm 29 \text{ mmol TCO}_2 \text{ m}^{-2} \text{ d}^{-1}$  during the first visit to station A3 and decreased to  $84 \pm 6 \text{ mmol O}_2 \text{ m}^{-2} \text{ d}^{-1}$  and  $-101 \pm 40 \text{ mmol TCO}_2 \text{ m}^{-2} \text{ d}^{-1}$  during the last occupation of station A3 (Fig. 5A and B). At the HNLC site C11, GCP ranged between  $30 \pm 15$  and  $38 \pm 13 \text{ mmol O}_2 \text{ m}^{-2} \text{ d}^{-1}$  (Fig. 5C). For NCP, euphotic zone depth-integrated values ranged between  $64 \pm 10$  and  $92 \pm 14 \text{ mmol O}_2 \text{ m}^{-2} \text{ d}^{-1}$  and between  $-43 \pm 45$  and  $-105 \pm 32 \text{ mmol TCO}_2 \text{ m}^{-2} \text{ d}^{-1}$  for the first three visits to station A3, and integrated NCP was  $-72 \pm 7 \text{ mmol O}_2 \text{ m}^{-2} \text{ d}^{-1}$  and  $64 \pm 47 \text{ mmol TCO}_2 \text{ m}^{-2} \text{ d}^{-1}$  during the fifth occupation (Fig. 5A and B). At the HLNC site C11, euphotic zone integrated NCP ranged between  $0 \pm 13$  and  $5 \pm 12 \text{ mmol O}_2 \text{ m}^{-2} \text{ d}^{-1}$  for the three visits (Fig. 5C). DCR integrated to the euphotic zone ranged from  $-35$  to  $-43 \text{ mmol O}_2 \text{ m}^{-2} \text{ d}^{-1}$  and from  $27$  to  $38 \text{ mmol TCO}_2 \text{ m}^{-2} \text{ d}^{-1}$  during the first three visits to station A3 and amounted to  $-155 \text{ mmol O}_2 \text{ m}^{-2} \text{ d}^{-1}$  and  $160 \text{ mmol TCO}_2 \text{ m}^{-2} \text{ d}^{-1}$  during the last visit (A3-5, Fig. 5A and B). At the HLNC site C11, euphotic depth integrated values for DCR ranged between  $-30$  and  $-35 \text{ mmol O}_2 \text{ m}^{-2} \text{ d}^{-1}$  (Fig. 5C).

GCP normalized to chlorophyll *a* concentrations amounted to  $0.11 \text{ mmol O}_2 (\text{mg chl } a)^{-1} \text{ h}^{-1}$  during the first and third visits to station A3 and decreased to  $0.07$  and  $0.06 \text{ mmol O}_2 (\text{mg chl } a)^{-1} \text{ h}^{-1}$  during the fourth and fifth occupations.

The GCP:DCR ratio ranged between  $2.5$  and  $3.1$  during the first three visits to station A3 indicating that GCP exceeded DCR. During the fifth occupation to station A3, however, the GCP:DCR ratio was  $0.5$ . At the HLNC site C11, DCR, and GCP were close to balance as indicated by a mean ( $\pm$ SD) ratio of  $1.1 \pm 0.08$  ( $n = 3$ ).

### 3.3. RQ and PQ

Based on the relationship between the  $\text{O}_2$  and  $\text{TCO}_2$  rates, we determined the RQ and PQ for the four visits at station A3. Mean ( $\pm$ SD) PQ and RQ values were  $1.03 \pm 0.86$  and  $1.01 \pm 1.14$  (Table 2).

## 4. Discussion

Net autotrophic metabolism dominated during the third month of the Kerguelen bloom, thus the microplankton community represented a potential sink of atmospheric carbon dioxide. The low community respiration relative to gross production indicates that a large fraction of photosynthetically fixed carbon was available for meso-

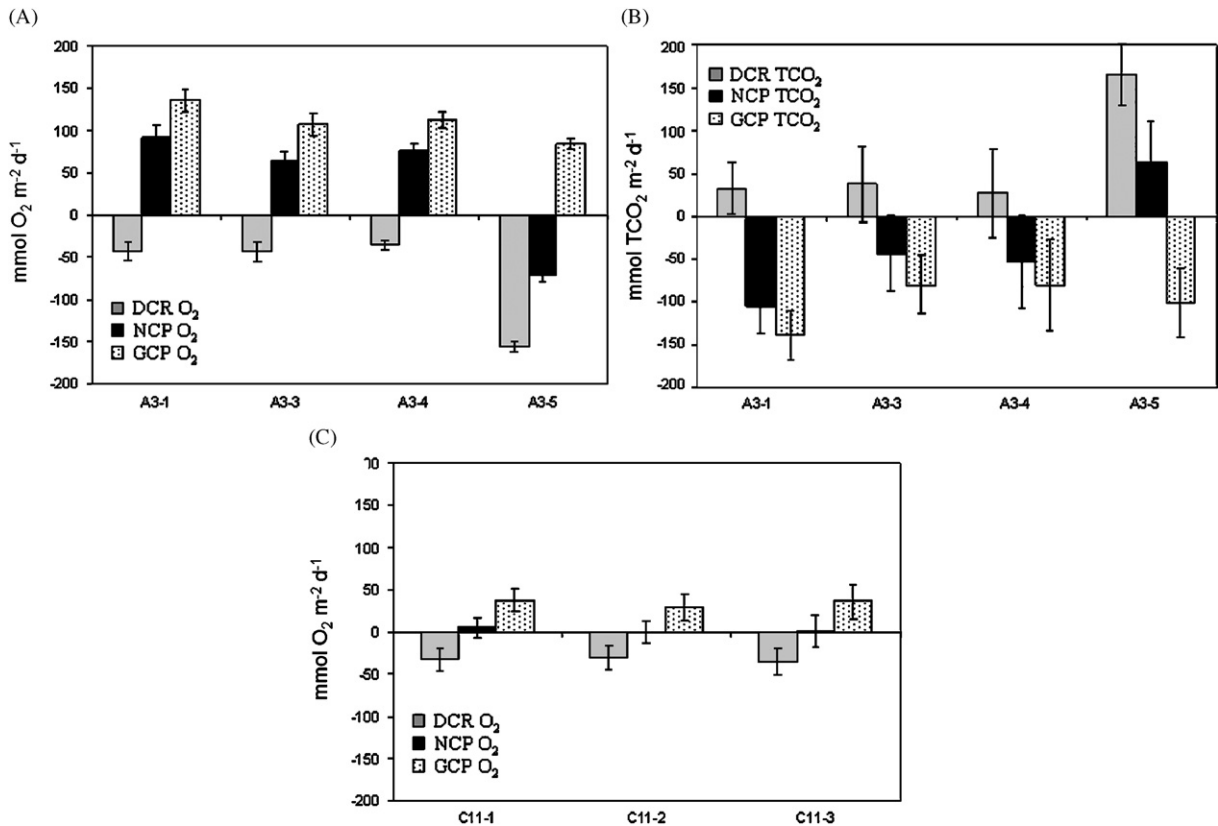


Fig. 5. Fluxes of gross community production (GCP), dark community respiration (DCR) and net community production (NCP) determined for  $\text{O}_2$  rates (A,C) and  $\text{TCO}_2$  rates (B) integrated to the euphotic zone at station A3 (upper panel) and station C11 (lower panel). Mean values  $\pm$  SE are given.

zooplankton grazing and export to the ocean interior. Towards the final bloom stage, however, community respiration markedly increased resulting in a shift to net heterotrophic pelagic metabolism. This suggests that the phasing of production and respiration is important for the fate of at least a part of the organic carbon produced during the Kerguelen bloom.

#### 4.1. Primary production during phytoplankton blooms in the Southern Ocean

The Southern Ocean is poorly characterized with respect to planktonic metabolism. Exceptions are coastal regions around Antarctica where several studies have investigated temporal and spatial variability in the metabolic balance (Blight, 1996 and references therein; Robinson et al., 1999; Agustí et al., 2004 and references therein). Our aim to place the rates of net and GCP determined above and off the Kerguelen plateau into a larger context is therefore limited to the comparison of production based on  $^{14}\text{C}$  and  $^{13}\text{C}$  incorporation. During the KEOPS-cruise, primary production determined from  $^{13}\text{C}$  incorporation ranged between 81 and 89  $\text{mmol C m}^{-2} \text{d}^{-1}$  and between 16 and 21  $\text{mmol C m}^{-2} \text{d}^{-1}$  at stations A3 and C11, respectively (Table 3, Mosseri et al., 2008). Thus,  $^{13}\text{C}$  primary production was similar to NCP during the first occupation of station A3, but closer to GCP during the following three visits (Table 3). By contrast, production estimated from  $^{14}\text{C}$  incorporation and P/I curves gave substantially higher values within the Kerguelen bloom (72–198  $\text{mmol C m}^{-2} \text{d}^{-1}$ ,

B. Griffiths, unpublished data). These estimates of primary production determined above the Kerguelen bloom are in the range of those obtained during the spring phytoplankton bloom in the Polar Front Zone of the Indian Sector of the Southern Ocean ( $^{14}\text{C}$  incorporation, mean 100  $\text{mmol C m}^{-2} \text{d}^{-1}$ ) (Quéguiner et al., 1997). An investigation of primary productivity across the Pacific Sector of the Southern Ocean (170°W from 54 to 72°S) revealed a minor variability (mean  $67 \pm 5 \text{ mmol C m}^{-2} \text{d}^{-1}$ ) in spring primary production ( $^{14}\text{C}$  incorporation) despite the different subsystems studied (Hiscock et al., 2003). These authors suggest that the mixing with iron-rich upper circumpolar deep water regulates the phytoplankton blooms (Hiscock et al., 2003). Controlled mesoscale iron additions to surface waters in the Southern Ocean yielded rates of primary production ( $^{14}\text{C}$  incorporation) varying between 66 and 120  $\text{mmol C m}^{-2} \text{d}^{-1}$  inside the Fe-patch during EisenEx (Gervais et al., 2002), SOIREE (Gall et al., 2001) and SOFeX (Coale et al., 2004) 2–3 weeks after bloom initiation. Thus, the rates of production during the third month of the Kerguelen bloom are in the range of those reported for other Southern Ocean open-ocean sites that experience naturally occurring or deliberately induced phytoplankton blooms. Whether these rates represent phytoplankton net growth is difficult to evaluate, as concurrent rates of community respiration are not available.

Based on the dissolved inorganic carbon (DIC) budget, Jouandet et al. (2008) determined the NCP of the Kerguelen bloom on a seasonal time scale. At station A3, the DIC budget yielded an NCP ( $99 \pm 37 \text{ mmol C m}^{-2} \text{d}^{-1}$ ) similar to that determined by *in vitro* measurements during the first visit to station A3 ( $109 \pm 44 \text{ mmol C m}^{-2} \text{d}^{-1}$ , Table 3). By contrast, estimates of NCP varied substantially between the two approaches at station C11. NCP determined by the seasonal DIC budget amounted to  $25 \pm 8 \text{ mmol C m}^{-2} \text{d}^{-1}$ , while *in vitro* measurements revealed negative estimates of NCP ( $-8 \pm 13 \text{ mmol C m}^{-2} \text{d}^{-1}$ ). The difference in NCP as derived by these approaches is clearly due to the different time scales of the measurements. *In vitro* rate measurements are representative of autotrophic and heterotrophic dynamics on the time scale of

Table 2  
Photosynthetic (PQ) and respiratory quotients (RQ)

Station	PQ ( $n = 6$ )	RQ ( $n = 6$ )
A3-1	$0.82 \pm 0.37$	$1.29 \pm 0.85$
A3-3	$1.28 \pm 0.31$	$0.89 \pm 0.61$
A3-4	$1.26 \pm 0.66$	$0.83 \pm 0.42$
A3-5	$0.77 \pm 0.28$	$1.03 \pm 0.18$

Mean values  $\pm$  SE are given.

Table 3  
Comparison of mixed layer depth integrated primary production determined from  $\text{TCO}_2$  fluxes,  $^{13}\text{C}$  and  $^{14}\text{C}$  incorporation (P/I curves)

Station	Zm (m)	NCP ( $\text{mmol C m}^{-2} \text{d}^{-1}$ )	GCP ( $\text{mmol C m}^{-2} \text{d}^{-1}$ )	$^{13}\text{C}$ -PP ( $\text{mmol C m}^{-2} \text{d}^{-1}$ ) <sup>b</sup>	$^{14}\text{C}$ -PP ( $\text{mmol C m}^{-2} \text{d}^{-1}$ ) <sup>c</sup>
A3-1	$52 \pm 12$	$109 \pm 44$	$138 \pm 29$	88	198
A3-3	$51 \pm 14$	$28 \pm 53$	$80 \pm 34$	85	156
A3-4	$79 \pm 20$	$29 \pm 98$	$80 \pm 53$	89	137
A3-5	$84 \pm 5$	$-174 \pm 86$	$101 \pm 40$	81	72
C11-1 <sup>a</sup>	$73 \pm 13$	$2 \pm 13$	$25 \pm 8$	21	32
C11-2 <sup>a</sup>	$73 \pm 13$	$-1 \pm 15$	$20 \pm 10$	16	18
C11-3 <sup>a</sup>	$56 \pm 1$	$8 \pm 12$	$20 \pm 8$	19	14

Production values were integrated to the mixed layer depth applying a linear model.

Zm—mixed layer depth.

<sup>a</sup>Values are based on  $\text{O}_2$  fluxes, converted to C-units applying an RQ of 1 and a PQ of 1.2 (see text).

<sup>b</sup>Data are from Garcia in Mosseri et al. (2008).

<sup>c</sup>Data are from Griffiths (unpublished data).

hours to days, whereas the seasonal budget is an integrative measure over weeks to months. The *in vitro* measurements do not take into account the possible time lags between production and respiration of organic carbon. The NCP determined on the basis of the seasonal DIC budget (Jouandet et al., 2008) is in the higher range of those reported from mesoscale iron addition experiments (31–38 and 70 mmol C m<sup>-2</sup> d<sup>-1</sup> for EisenEx and SOIREE, respectively; Bakker et al., 2005).

#### 4.2. What induces net heterotrophy at the final bloom stages?

The remarkably constant rates of community respiration during the first three visits to station A3 indicate that the variability in the phytoplankton GCP was the main factor controlling the variability in NCP (Fig. 3). During the last visit at the bloom station, however, a substantial increase in DCR was observed resulting in a shift to net heterotrophic metabolism. To better understand this shift in NCP, we will discuss the factors controlling production and respiration.

Quantifying the contribution of the autotrophic and heterotrophic plankton components to community respiration is not possible for the present study; however, the factors controlling autotrophic and heterotrophic activity could help to understand the observed changes in the ratio of GCP to DCR. The main controlling factors of autotrophic activity are phytoplankton biomass, the supply of inorganic nutrients and the irradiance regime. During the survey period no changes in the concentration of inorganic nutrients were detectable above the Kerguelen plateau (Table 1) and daily PAR varied by up to 2-fold over the sampling period (B. Griffiths, unpublished data). Using a production versus irradiance model (Jassby and Platt, 1976) and physiological photosynthetic parameters (B. Griffiths, pers. comm.), we estimated that the 2-fold increase in the daily PAR induces a maximum increase of 40% in GCP. However, the daily PAR during the first visit (A3-1) was equivalent to that during the last visit (A3-5). We can therefore conclude that PAR was not the main factor controlling the variability in GCP at station A3. Phytoplankton biomass (chl *a*) decreased by 1.5-fold between the fourth and the fifth visit to station A3 (Table 1). Similarly, <sup>14</sup>C-primary production based on P/I curves revealed a pronounced decrease between the fourth and the fifth visit to station A3, while only a minor decrease in <sup>13</sup>C-primary production was observed (Table 3). The former estimate of primary production, based on short-term (1-h) incubations, is indicative of a change in the carbon assimilation rate, incorporation, based on 24-h incubations at set PAR levels does not necessarily reflect the physiological state of the cell. The decrease in the specific GCP and in the Fv/Fm ratio (Timmermans, pers. comm.) further support the notion of the degradation of the physiological status of the phytoplankton community during the fifth visit to station A3.

This could result in a higher autotrophic respiration thereby increasing overall plankton respiration during the decline of the phytoplankton bloom.

The observed shift to net heterotrophic plankton metabolism was not related to any major change in the microplankton community structure. Diatoms were the major biomass component during all visits (82% of total microplankton community biomass), while biomass contributions of heterotrophic bacteria (5%), nanoflagellates (4%), and ciliates (<1%) were minor (Christaki et al., 2008). Thus, changes in the activities of the different components of the microplankton community are most likely to explain the observed increase in community respiration. Concurrently, pronounced changes in the major species composition were observed. *Chaetoceros* spp. dominated the phytoplankton biomass during the first and second visit, while *Eucampia antarctica* was the major biomass contributor during the fourth and the fifth visit (Armand et al., 2008). These two species present different surface-to-volume ratios, respectively, of 0.7 and 0.3 for *Chaetoceros* spp and *E. antarctica*, respectively (Cornet-Barthaux et al., 2007), further suggesting an increased contribution of autotrophic respiration to community respiration (Tang and Peters, 1995).

The supply of an allochthonous source of organic carbon to sustain the high plankton community respiration rates during our last visit to station A3 is unlikely. The horizontal current is less than 8 cm s<sup>-1</sup> in the vicinity of station A3 (Park et al., 2008) suggesting that horizontal advection is insufficient to transport a significant amount of allochthonous organic material to station A3. The observation that phytoplankton biomass did not accumulate during the survey period (Uitz et al., 2008; Armand et al., 2008) supports the idea that photosynthetically produced organic matter was continuously removed from the mixed layer, sedimentation and mesozooplankton grazing being the predominant processes. Furthermore, we did not observe any accumulation in dissolved organic carbon in the mixed layer at station A3 during the survey period (Jouandet et al., 2008). This indicates a rapid utilization of organic matter, most likely due to its high bio-reactivity and the availability of inorganic nutrients. A marked increase in mineralization, as shown by our DCR measurements, is also indicated by a shift from NO<sub>3</sub><sup>-</sup> to NH<sub>4</sub><sup>+</sup> uptake (Garcia pers. comm.). NH<sub>4</sub><sup>+</sup> uptake increased from 39% to 75% of the nitrogen uptake between the fourth and fifth visit to station A3. Further, the NH<sub>4</sub><sup>+</sup> regeneration flux within the microbial community doubled between the first and last visit at station A3 (Mosseri et al., 2008).

PQ and RQ are representative for the coupling between the carbon and oxygen metabolism during photosynthetic and respiratory processes, respectively. The PQ reported in the present study are in the range of theoretical values for the open ocean (Laws, 1991; Williams and Robertson, 1991). The RQ is representative of the full oxidation of the organic material by the microbial community and it varies



according to the quality of the organic material, i.e. the O/C ratio of the organic substrate. Theoretical values range from 0.66 to 1.3 depending on the substrate (Lenhinger et al., 1994) and *in situ* derived values for the stoichiometric composition of organic matter vary between 0.67 (Shaffer, 1996), 0.71 (Takahashi et al., 1985), 0.77 (Redfield et al., 1963), and up to 1.06 (Minster and Boulahdid, 1987). Our RQ ( $0.83 \pm 0.42$  to  $1.29 \pm 0.85$ , Table 2) are similar to those determined with the same technique for coastal Antarctic waters ( $0.88 \pm 0.14$ , Robinson et al., 1999) and for the Arabian Sea ( $1.64 \pm 0.26$ , Robinson and Williams, 1999). Insight into the composition of organic matter relative to the *in situ* variation in RQ is needed to gain a better understanding of the coupling between oxygen and carbon metabolism, which may provide insight into the respiration dynamics.

Based on size-fractionation experiments, the heterotrophic bacterial contribution to community respiration at station A3 was estimated to be  $\approx 90\%$  and  $\approx 40\%$  during the third and fourth visit, respectively, while it accounted for only 6% of DCR during the fifth occupation (Obernosterer et al., 2008). Size fractionation, however, excludes particle-attached bacteria. Higher abundances and activities of particle-attached bacteria could also contribute to the observed increase in DCR towards the decline of the bloom. Diatoms can produce high amounts of exopolymers, in particular during the senescent phase (Decho, 1990). As a result, diatom cells aggregate forming microhabitats that are rapidly colonized by heterotrophic bacteria. Besides, particularly high aminopeptidase activities were noticed above the Kerguelen plateau (Christaki and Van Wambeke, unpublished data). This appears to be a general phenomenon in Antarctic waters compared to other oceanic provinces (Christian and Karl, 1998; Arrieta et al., 2004). Bidle and Azam (2001) described the key role of aminopeptidase for hydrolyzing the peptide wall of diatoms, allowing solubilization of siliceous material. This first step seems important in order for bacteria to access the intracellular contents of diatoms. The high load of particulate organic matter above the Kerguelen plateau, and the biological activity on aggregates trapped in the BOD bottles probably contributed substantially to the enhanced respiration rates. A similar observation is reported from the decline of a phytoplankton bloom induced by mesoscale Fe-addition in the subarctic Pacific, where bacterial activity was suggested to have a major contribution to overall particulate organic carbon mineralization (Boyd et al., 2004). Also an increase in POC stock with time was observed (Jouandet et al., 2008), with no apparent changes in the living biomass stock (Christaki et al., 2008), suggests an increase in the detritus load.

These arguments suggest that net heterotrophy could be partially attributable to the phasing of production and respiration above the Kerguelen plateau (Aristegui and Harrison, 2002; Blight et al., 1995).

Microplankton respiration clearly dominated overall plankton respiration. Based on the mesozooplankton

biomass and an allometric relationship (Atkinson et al., 1996), respiration rates in the mixed-layer depth amounted to roughly 10 and  $2 \text{ mmol C m}^{-2} \text{ d}^{-1}$  at stations A3 and C11, respectively (Carlotti et al., 2008). Mesozooplankton respiration thus accounted for roughly 10% of overall plankton respiration both above and off the Kerguelen plateau.

The continuous supply of iron and major nutrients above the Kerguelen plateau (Blain et al., 2007) clearly stimulated production and respiration. Based on the build-up of a large stock of phytoplankton biomass, we can safely assume that net autotrophy dominated planktonic metabolism during the spring phytoplankton bloom above the Kerguelen plateau. Rates of production are in the range of those reported previously for spring phytoplankton blooms in the Southern Ocean; however, data on NCP, an indicator of the organic matter stored in surface waters potentially available for export to the deep ocean thus far are scarce. The high rates of NCP determined in the present study and the observed drawdown of  $\text{pCO}_2$  during the Kerguelen bloom (Blain et al., 2007) point to the potential importance of planktonic metabolism for the absorption of atmospheric  $\text{CO}_2$ . The net production of carbon over a relatively long time period (3 months) sustained a high mesozooplankton biomass (Carlotti et al., 2008) and resulted in substantial export of particulate organic matter below the mixed layer (Savoie et al., 2008).

## Acknowledgments

We thank the captain and the crew of the R.V. *Marion Dufresne* and the chief scientists S. Blain and B. Quéguiner for their enthusiastic support aboard. Brian Griffiths is acknowledged for providing  $^{14}\text{C}$  GPP, daily PAR and physiological photosynthesis parameters, Julia Uitz for providing chlorophyll *a* data. The three reviewers are greatly acknowledged for helping us improving this MS. This work was supported by the French National Program PROOF (CNRS/INSU) and the Institut Polaire Emile Victor (IPEV).

## References

- Agustí, S., Satta, M.P., Mura, M.P., 2004. Summer community respiration and pelagic metabolism in upper surface Antarctic waters. *Aquatic Microbial Ecology* 35, 197–205.
- Aristegui, J., Harrison, Y.W.G., 2002. Decoupling of primary production and respiration in the ocean: implications for regional carbon studies. *Aquatic Microbial Ecology* 29, 199–209.
- Armand, L., Cornet-Barthau, V., Mosseri, J., Quéguiner, B., 2008. Late summer diatom biomass and community structure on and around the naturally iron-fertilized Kerguelen plateau in the Southern Ocean. *Deep-Sea Research II*, this issue [doi:10.1016/j.dsr2.2007.12.031].
- Arrieta, J.M., Weinbauer, M., Lute, C., Herndl, G.J., 2004. Response of bacterioplankton to iron fertilisation in the southern Ocean. *Limnology and Oceanography* 49, 799–808.
- Atkinson, A., Shreeve, R.S., Pakhomov, E.A., Priddle, J., Blight, S.P., Ward, P., 1996. Zooplankton response to a phytoplankton bloom near

- South Georgia, Antarctica. *Marine Ecology—Progress Series* 144, 195–210.
- Bakker, D.C.E., Bozec, Y., Nightingale, P.D., Goldson, L.E., Messias, M.J., De Baar, H.J.W., Liddicoat, M.I., Skjelvan, I., Strass, V., Watson, A.J., 2005. Iron and mixing affect biological carbon uptake in Soiree and Eisenex, two Southern Ocean iron fertilisation experiments. *Deep-Sea Research Part I* 52, 1001–1019.
- Bidle, K.D., Azam, F., 2001. Bacterial control of silicon regeneration from diatom detritus: significance of bacterial ectohydrolases and species identity. *Limnology and Oceanography* 46 (7), 1606–1623.
- Blain, S., Tréguer, P., Belviso, S., Bucciarelli, E., Denis, M., Desabre, S., Fiala, M., Lefevre, J., Martin Jézéquel, V., Marty, J.C., Mayzaud, P., Razouls, S., 2001. Biogeochemical study of an island mass effect in the context of the iron hypothesis in the Southern Ocean. *Deep-Sea Research I* 48, 163–187.
- Blain, S., Quéguiner, B., Armand, L.K., Belviso, S., Bombled, B., Bopp, L., Bowie, A., Brunet, C., Brussaard, C., Carlotti, F., Christaki, U., Shreeve, R.S., Corbière, A., Durand, I., Ebersbach, F., Fuda, J.L., Garcia, N., Gerringa, L., Griffiths, B., Guigue, C., Guillermin, C., Jacquet, S., Jeandel, C., Laan, P., Lefèvre, D., Lomonaco, C., Maliet, A., Mosseri, J., Obernosterer, I., Park, H.Y., Picheral, M., Pondaven, P., Remenyi, T., Sandroni, V., Sarthou, G., Savoye, N., Scouarnec, L., Souhaut, M., Thuiller, D., Timmermans, K., Trull, T., Uitz, J., Van-Beek, P., Veldhuis, M., Vincent, D., Viollier, E., Vong, L., Wagener, T., 2007. Impact of natural iron fertilisation on carbon sequestration in the Southern Ocean. *Nature* 446, 1070–1074.
- Blain, S., Sarthou, G., Laan, P., 2008. Distribution of dissolved iron during the natural iron fertilisation experiment KEOPS (Kerguelen Plateau, Southern Ocean). *Deep-Sea Research II*, this issue [doi:10.1016/j.dsr2.2007.12.028].
- Blight, S.P., 1996. Microbial metabolism and temperature. Comparative studies in the Southern Ocean and a temperate coastal ecosystem. Ph.D. Thesis, University of Wales, Bangor, p. 215.
- Blight, S.P., Bentley, T.L., Lefevre, D., Robinson, C., Rodrigues, R., Rowlands, J., Williams, P.J.leB., 1995. The phasing of autotrophic and heterotrophic planktonic metabolism in a temperate coastal ecosystem. *Marine Ecology—Progress Series* 128, 61–75.
- Boyd, P.W., Watson, A., Law, C.S., Abraham, E., Trull, T., Murdoch, R., Bakker, D.C.E., Bowie, A.R., Charette, M., Croot, P., Downing, K., Frew, R., Gall, M., Hadfield, M., Hall, J., Harvey, M., Jameson, G., La Roche, J., Liddicoat, M., Ling, R., Maldonado, M., McKay, R.M., Nodder, S., Pickmere, S., Pridmore, R., Rintoul, S., Safi, K., Sutton, P., Strzepek, R., Tannenberger, K., Turner, S., Waite, A., Zeldis, J., 2000. Mesoscale iron fertilisation elevates phytoplankton stocks in the polar Southern Ocean. *Nature* 407, 695–702.
- Boyd, P.W., Law, C.S., Wong, C.S., Nojiri, Y., Tsuda, A., Lefevre, M., Takeda, S., Rivkin, R., Harrison, P.J., Strzepek, R., Gower, J., McKay, R.M., Abraham, E., Arychuk, M., Barwell-Clarke, J., Crawford, W., Crawford, D., Hale, M., Harada, K., Johnson, K., Kiyosawa, H., Kudo, I., Marchetti, A., Miller, W., Needoba, J., Nishioka, J., Ogawa, H., Page, J., Robert, M., Saito, H., Sastri, A., Sherry, N., Soutar, T., Sutherland, N., Taira, Y., Whitney, F., Wong, S.K.E., Yoshimura, T., 2004. The decline and fate of an iron-induced Subarctic phytoplankton bloom. *Nature* 428, 549–553.
- Buesseler, K.O., Andrews, J.E., Pike, S.M., Charette, M.A., 2004. The effects of iron fertilisation on carbon sequestration in the Southern Ocean. *Science* 304, 414–417.
- Carlotti, F., Thibault-Botha, D., Nowaczyk, A., Lefèvre, D., 2008. Zooplankton community structure, biomass and role in carbon fluxes during the second half of a phytoplankton bloom in the eastern sector of the Kerguelen shelf (January–February 2005). *Deep-Sea Research II*, this issue [doi:10.1016/j.dsr2.2007.12.010].
- Christaki, U., Obernosterer, I., Van Wambeke, F., Veldhuis, M.J.W., Garcia, N., Catala, P., 2008. Microbial food web structure in a naturally iron fertilized area in the Southern Ocean (Kerguelen Plateau). *Deep-Sea Research II*, this issue [doi:10.1016/j.dsr2.2007.12.009].
- Christian, J.R., Karl, D.M., 1998. Ectoaminopeptidase specificity and regulation in Antarctic marine pelagic microbial communities. *Aquatic Microbial Ecology* 15, 303–310.
- Coale, K.H.K.S., Johnson, K.S., Chavez, F.P., Buesseler, K.O., Barber, R.T., Brzezinski, M.A., Cochlan, W.P., Millero, F.J., Falkowski, P.J., Bauer, J.E., Wanninkhof, R.H., Kudela, R.M., Altabet, M.A., Hales, B.E., Takahashi, T., Landry, M.R., Bidigare, R.R., Wang, X., Chase, Z., Stratton, P.G., Friederich, G.E., Gorbunov, M.Y., Lance, V.P., Hilding, A.K., Hiscock, M.R., Demarest, M., Hiscock, W.T., Sullivan, K.F., Tanner, S.J., Gordon, R.M., Hunter, C.N., Elrod, V.A., Fitzwater, S., Jones, J.L., Tozzi, S., Koblizek, M., Roberts, A.E., Herndon, J., Brewster, J., Ladizinsky, N., Smith, G., Cooper, D., Timothy, D., Brown, S.E., Selph, K.E., Sheridan, C.C., Twining, B.S., Johnson, Z.I., 2004. Southern ocean iron enrichment experiment: carbon cycling in high- and low-Si waters. *Science* 304 (5669), 408–414.
- Cornet-Barthaux, V., Armand, K.L., Quéguiner, B., 2007. Biovolume and biomass measurements of key Southern Ocean diatoms. *Aquatic Microbial Ecology* 48, 295–308.
- Decho, A.W., 1990. Microbial exopolymer secretions in ocean environments: their role(s) in food webs and marine processes. *Oceanography and Marine Biology—Annual Review* 28, 73–L 53.
- DOE, 1994. In: Dickson, A.G., Goyet, C. (Eds.), *Handbook of Methods for the Analysis of the Various Parameters of the Carbon dioxide System in Sea Water*, Version 2 (Ornl/Cdiac-74).
- Gaarder, T., Gran, H.H., 1927. Investigations of the production of plankton in the Oslo fjord. *Rapports et Proces-Verbaux des Reunions, Conseil International pour l'Exploration de la Mer* 42, 1–48.
- Gall, M.R., Strzepek, R., Maldonado, M., Boyd, P.W., 2001. Phytoplankton processes. Part 2: rates of primary production and factors controlling algal growth during the Southern Ocean iron release experiment (Soiree). *Deep-Sea Research II* 48, 2571–2590.
- Gervais, F., Riebesell, U., Gorbunov, M.Y., 2002. Changes in primary productivity and chlorophyll *a* in response to iron fertilisation in the Southern Polar Frontal Zone. *Limnology and Oceanography* 47, 1324–1335.
- Hiscock, M.R., 2004. Regulation of primary productivity in the Southern Ocean. Ph.D. Thesis, Duke University, 174pp.
- Hiscock, M.R., Marra, J., Smith Jr., W.O., Goericke, R., Measures, C., Vink, S., Olson, R.J., Sosik, H.M., Barber, R.T., 2003. Primary productivity and its regulation in the Pacific Sector of the Southern Ocean. *Deep-Sea Research II* 50, 533–558.
- Jassby, A.D., Platt, T., 1976. Mathematical formulation of the relationship between photosynthesis and light for phytoplankton. *Limnology and Oceanography* 21, 540–547.
- Johnson, K.M., Wills, K.D., Butler, D.B., Johnson, W.K., Wong, C.S., 1993. Coulometric total carbon dioxide analysis for marine studies: maximizing the performance of an automated gas extraction system and coulometric detector. *Marine Chemistry* 44, 167–188.
- Jouandet, M.P., Blain, S., Metz, N., Brunet, C., Trull, T., Obernosterer, I., 2008. A seasonal carbon budget for a naturally fertilized bloom over the Kerguelen plateau in the Southern Ocean. *Deep-Sea Research II*, this issue [doi:10.1016/j.dsr2.2007.12.037].
- Karl, D.M., 1993. Microbial processes in the southern oceans. In: Friedman, E.I. (Ed.), *Antarctic Microbiology*. Wiley-Liss, pp. 11–63.
- Kudo, I., Noiri, Y., Imai, K., Nojiri, Y., Nishioka, J., Tsuda, A., 2005. Primary productivity and nitrogenous nutrient assimilation dynamics during the Subarctic Pacific iron experiment for ecosystem dynamics study. *Progress in Oceanography* 64, 207–221.
- Laws, E.A., 1991. Photosynthetic quotient, new production and net community production in the open ocean. *Deep-Sea Research* 38, 143–167.
- Lenhinger, A.L., Nelson, D.L., Cox, M.M., 1994. *Principes de biochimie*, 2eme ed. Flammarion, 1035pp.
- McCartney, M.S., Donohue, K.A., 2007. A deep cyclonic gyre in the Australian-Antarctic basin. *Progress in Oceanography* 75 (4), 675–750.
- Minster, J.F., Boulahdid, M., 1987. Redfield ratios along isopycnal surfaces—a complementary study. *Deep-Sea Research I* 34, 1981–2003.

- Mosseri, J., Quéguiner, B., Armand, L., Cornet-Barthau, V., 2008. Impact of iron on silicon utilization by diatoms in the Southern Ocean: a case of Si/N cycle decoupling in a naturally iron-enriched area. *Deep-Sea Research II*, this issue [doi:10.1016/j.dsr2.2007.12.003].
- Obernosterer, I., Christaki, U., Lefèvre, D., Catala, P., Van Wambeke, F., Le Baron, P., 2008. Rapid bacterial remineralization of organic carbon produced during a phytoplankton bloom induced by natural iron fertilization in the Southern Ocean. *Deep-Sea Research II*, this issue [doi:10.1016/j.dsr2.2007.12.005].
- Park, Y.-H., Gambèroni, L., 1997. Cross frontal injections of Antarctic intermediate water and Antarctic bottom water in the Crozet Basin. *Deep-Sea Research II* 44, 963–986.
- Park, Y.-H., Gambèroni, L., Charriaud, E., 1991. Frontal structure, transport and variability of the Antarctic Circumpolar Current in the South Indian Ocean sector, 40–80°E. *Marine Chemistry* 35, 45–62.
- Park, Y.-H., Gambèroni, L., Charriaud, E., 1993. Frontal structure, water masses, and circulation in the Crozet Basin. *Journal of Geophysical Research* 98, 12361–12385.
- Park, Y.-H., Charriaud, E., Ruiz Pino, D., Jeandel, C., 1998. Seasonal and interannual variability of the mixed-layer properties and steric height at station KERFIX, southwest of Kerguelen. *Journal of Marine Systems* 17, 233–247.
- Park, Y.H., Fuda, J.L., Durand, I., Naveira Garabato, A.C., 2008. Internal tides and vertical mixing over the Kerguelen Plateau. *Deep-Sea Research II*, this issue [doi:10.1016/j.dsr2.2007.12.027].
- Pomeroy, L.R., Deibel, D., 1986. Temperature regulation of bacterial activity during the spring bloom in Newfoundland coastal waters. *Science* 233, 359–361.
- Quéguiner, B., Tréguer, P., Peeken, I., Scharek, R., 1997. Biogeochemical dynamics and the silicon cycle in the Atlantic sector of the Southern Ocean during austral spring 1992. *Deep-Sea Research II* 44, 69–89.
- Redfield, A.C., Ketchum, B.H., Richards, F.A., 1963. The influence of organisms on the composition of sea-water. In: Hill, M.N. (Ed.), *The Sea*, vol. 2. Wiley-Interscience, New York, pp. 26–77.
- Robinson, C., Williams, P.J.leB., 1999. Plankton net community production and dark community respiration in the Arabian Sea during September 1994. *Deep-Sea Research II* 46, 745–766.
- Robinson, C., Archer, S.D., Williams, P.J.leB., 1999. Microbial dynamics in coastal waters of East Antarctica: plankton production and respiration. *Marine Ecology—Progress Series* 180, 23–36.
- Roquet, F., Park, Y.-H., Guinet, C., Charassin, J.-B., 2008. Observations of the Fawn Trough Current over the Kerguelen Plateau from instrumented elephant seals. *Journal of Marine Systems*, in press.
- Savoie, N., Trull, T.W., Jacquet, S., Navez, J., Dehairs, F., 2008. <sup>234</sup>Th-based export fluxes during a natural iron fertilisation experiment in the Southern Ocean. *Deep-Sea Research II*, this issue [doi:10.1016/j.dsr2.2007.12.036].
- Shaffer, G., 1996. Biogeochemical cycling in the global ocean. 2. New production, Redfield ratios and remineralisation in the organic pump. *Journal of Geophysical Research* 101, 3723–3745.
- Sullivan, C.W., Arrigo, K.R., McClain, C.R., Comiso, J.C., Firestone, J., 1993. Distribution of phytoplankton blooms in the Southern Ocean. *Science* 262, 1832–1837.
- Takahashi, T., Broecker, W.S., Langer, S., 1985. Redfield ratio based on chemical data from isopycnal surfaces. *Journal of Geophysical Research* 90, 6907–6924.
- Tang, E.P.Y., Peters, R.H., 1995. The allometry of algal respiration. *Journal of Plankton Research* 17, 303–315.
- Tréguer, P., LeCorre, P., 1975. Manuel d'analyse des sels nutritifs dans l'eau de mer. Utilisation de l'autoAnalyser II Technicon, second ed. Laboratoire de Chimie Marine, University of Bretagne Occidentale, Brest, France, pp. 1–110.
- Uitz, J., Claustre, H., Garcia, N., Griffiths, B., Ras, J., Sandroni, V., 2008. A phytoplankton class-specific primary production model applied to the Kerguelen Island Region (Southern Ocean). *Deep-Sea Research I*, submitted.
- Williams, P.J.leB., Jenkinson, N.W., 1982. A transportable micro-processor-controlled precise Winkler titration suitable for field station and shipboard use. *Limnology and Oceanography* 27, 576–584.
- Williams, P.J.leB., Robertson, J.E., 1991. Overall planktonic oxygen and carbon dioxide metabolisms: the problem of reconciling observations and calculations of photosynthetic quotients. *Journal of Plankton Research* 13 (Suppl.), 153–169.